Influence of an atomic grating on a magnetic Fermi surface

T. Greber, W. Auwärter, and J. Osterwalder

Physik-Institut, Universität Zürich, Winterthurerstrasse 190, CH-8057 Zürich, Switzerland

Version of, December 11, 2000

In "The Physics of Low Dimensional Systems", Ed. J.L. Morán-López, Plenum, New York, (2000).

Abstract

The spin–split electronic band structure of a ferromagnet–insulator interface is investigated. For the model system of a monolayer of hexagonal boron nitride on Ni(111) it is found that the insulator strongly influences the Fermi surface of the underlying ferromagnet. Angular resolved photoemission around the Fermi level provides direct insight into the modification of the electronic structure in the whole surface Brillouin zone. The commensurate *h*-BN overlayer acts as an atomic grating that produces strong surface umklapp processes. The intensity ratio between the spin–split s–p bands at the Fermi level is discussed in view of spin scattering asymmetry.

I. INTRODUCTION

The coupling between two magnets may be mediated by magnetic stray fields, electron tunneling or scattering. The electron mediated coupling mechanisms give rise to phenomena like the giant magneto resistance (GMR) i.e. an electrical resistance that strongly depends on the relative orientation of the magnetizations in two separated layers [1,2]. The physics of this coupling mechanism involves a spin dependent transmission coefficient for electrons moving parallel to or across the junction and is still under debate. In this context the knowledge of the Fermi surface and its evolution across the interface is of key importance.

The present paper shall contribute to a better understanding of spin dependent coupling in non–magnetic tunneling junctions. It foots on previous angular resolved photoemission experiments on clean nickel [3,4] and investigates the influence of a non-magnetic insulator on the Fermi surface. Cuts across the Fermi surfaces - as measured with photoemission [5] – of the bare Ni(111) and a monoatomic layer of hexagonal boron nitride on Ni(111) are compared. Perfect single layer *h*-BN films can be grown on Ni(111) and they are expected to behave like an insulator since the *h*-BN conduction band lies above the Fermi level [6]. Here it is shown that the non–magnetic insulator acts as a two-dimensional grating that multiplies states at the Fermi level and modifies the Ni bulk Fermi surface near the interface. The direct photoemission transitions from the exchange split s–p bands are exploited as spin polarized electron sources. A strong spin dependent emission asymmetry is found in comparing the down:up intensity ratio in Ni(111) and *h*-BN/Ni(111). It has to be emphasized that in this kind of experiments the spin has not to be measured – this would require a magnetized sample (and a spin detector) – but is resolved in k–space i.e. from photoemission angle and energy. The assignment of majority or minority spin is deduced from band structure calculations.

II. EXPERIMENTAL

The experiments were performed in a modified VG ESCALAB 220 photoelectron spectrometer with He Iα ($\hbar\omega$ = 21.2 eV) and He Iβ ($\hbar\omega$ = 23.1 eV) radiation [7,8]. These two photon energies are used in order to probe the same $k_{||}$-values at the same polar emission angles of the two samples which have different work functions [9]. In order to get the work function, spectra are taken at normal emission and a bias voltage of -9 V is applied to the sample in order to resolve the secondary electron emission cut off. From the width ΔE of the spectra the work function $\Phi = \hbar\omega - \Delta E$ is determined. For Ni(111) a work function of 5.1 eV and for *h*-BN/Ni(111) of 3.3 eV is found. The overall energy/momentum resolution was better than 50 meV/ 0.02 Å^{-1} FWHM and all presented data were taken at room temperature. $k_{||}$ is determined from the electron kinetic energy in the vacuum ($\equiv E_{kin}$) and the polar emission angle θ with respect to the optical surface: $k_{||} = sin(\theta)\sqrt{2m_e E_{kin}}/\hbar$. The sample preparation and characterization is described elsewhere [6,10]. It is found that *h*-BN forms perfect (1x1) commensurate monolayers on Ni(111).

III. RESULTS AND DISCUSSION

In Figure 1 Fermi surface maps of bare Ni(111) and *h*-BN/Ni(111) are shown. Essentially the photoemission intensity from the Fermi level is displayed on a linear gray scale for different emission angles in parallel projection. The maps correspond to a two dimensional cut across the k–space. In the free electron final state picture this two dimensional cut is the surface of a sphere with radius $k_f = \sqrt{2m_e(\hbar\omega - E_B - \Phi + U)}/\hbar$, where m_e is the free electron mass, $\hbar\omega$ the photon energy, E_B the binding energy ($\equiv$ 0 at the Fermi level), Φ the work function and U the inner potential (10.7 eV) [5]. The momentum of the photon is neglected and direct transitions obey the momentum coservation

$$\mathbf{k}_f = \mathbf{k}_i + \mathbf{G} \tag{1}$$

where $\mathbf{k}_f$ is the final state wave vector inside the solid, $\mathbf{k}_i$ the initial state wave vector and $\mathbf{G}$ is a reciprocal lattice vector of the three dimensional bulk lattice *and/or* two dimensional surface lattice. Clearly the Fermi surface map of Ni(111) has three fold rotational symmetry (Fig. 1a)). This makes sure that at least two atomic layers of nickel are probed. The Fermi surface map of *h*–BN/Ni(111) is as well three fold symmetric as it has to be expected from the atomic structure of the *h*–BN overlayer [10,11]. However, in comparing Figure 1a) and b) it can be seen that this insulating overlayer with no electronic states on the Fermi surface, strongly influences the shape of the Fermi surface and therefore the electronic coupling across the interface. The Fermi surface gets distorted and new features emerge. In the following we would like to highlight a particular spin–split feature from the s–p band and a surface umklapp. In Figures 1c) and d) the surface Brillouin zones of the corresponding maps in Figures 1a) and b) are shown. The two features that are further discussed are schematically sketched. There are the two slightly shifted $\wedge$ wedge like features in the second surface Brillouin zones along the $[\bar{1}\bar{1}2]$ direction and the features in the first surface Brillouin zone that are mimicked as a pair of "signal disks". Both features are mainly s–p derived bands [12]. They are cuts across the Fermi surface in the Γ_{002} (wedges) and the Γ_{111} (signal disks) bulk Brillouin zones close to the $L_{\frac{1}{2}\frac{1}{2}\frac{3}{2}}$ point. The signal disk like features change their shape in going from Ni(111) to *h*–BN/Ni(111). More importantly, in the *h*–BN/Ni(111) case (Figure 1b) and d)) it is seen that the three signal disk pairs are replicated three more times. They are shifted by a primitive reciprocal surface lattice vector $|\mathbf{Q}| = \frac{2\pi}{a}\frac{2}{\sqrt{3}} = 2.9\mathring{A}^{-1}$, where $a = 2.49\mathring{A}$ is the surface lattice constant. This is a surface umklapp process where the lattice vector $\mathbf{G}$ in the photoemission (see Eqn. 1) contains as well an element of the two dimensional reciprocal surface lattice. Note that the *h*–BN/Ni(111) sysem has still the same (1x1) symmetry as the clean Ni(111) surface. We take the occurence of such surface umklapps as an indication that the *h*–BN layer acts as an efficient grating for any electrons that cross this interface and that therefore such umklapps influence the tunneling characteristics of such junctions. Since the s–p bands are exchange split (see below) this will affect as well the spin asymmetry in the tunneling current.

In Figure 2 two cuts across the s–p wedges in the second surface Brillouin zone of Ni and h–BN/Ni(111) are displayed. For Ni (h–BN/Ni(111)) the same polar emission angle $\theta = 78°$ and the photon energies of 23.1 (21.2) eV were chosen in order to sample the same polar emission angles at the same $\mathbf{k}_{||}$ values [9]. The azimuthal emission angle was scanned $\pm 22°$ around the $(\bar{1}10)$ plane. The four peaks represent cuts across the Fermi–surface. They are characterized by their positions (δk_{ex} and $\delta k_{\uparrow\uparrow}$), their width γ and their area A. In Table I the left/right averaged quantities are summarized. The large group velocity (see Fig.3) identifies the bands as the s–p bands. The polarization can be assigned from comparison with band structure calculations where the inner peaks reflect the minority s–p band while the outer ones those with majority spin [12]. The exchange splitting δk_{ex} between the majority and the minority s–p band is 0.19 (0.16)$\mathring{A}^{-1}$. From the change in the angular splitting between the majority s–p bands ($\delta k_{\uparrow\uparrow}$) it can be seen that the Fermi surface gets slightly distorted by the h–BN interface. It has to be noted that the low work function of h–BN/Ni(111) with respect to the instrument work function may cause a slight violation of the nominal $k_{||}$ conservation. This is due to the electrosatic "lensing effect" since the different work functions induce electric fields in the vacuum. At these large polar emission angles we estimate that in the measured $k_{||}$ is overestimated by about 4%. Therefore the $\delta k_{\uparrow\uparrow}$ value of h–BN/Ni(111) has to be considered as slightly overestimated while control experiments with He Iα radiation on Ni(111) indicate that δk_{ex} is not affected by this shift in $k_{||}$.

The minority s–p band peak width $\gamma_{\downarrow}$ is about 30% larger than that of the majority bands ($\gamma_{\uparrow}$). This is in line with a shorter lifetime of minority excitations [13]. In three dimensional systems, however, the connection between the angular broadening and the initial– and finalstate liftimes is quite involved [14].

The intensity variation of the spin up / spin down doublets left and right from the high symmetry plane are caused by the loss of mirror symmetry due to the oblique incidence of the photons in our experimental set up. It provides a rough estimate for the change of the photoemission matrix element with respect to the orientation of the incoming light. In the

following the area ratio $\Upsilon = A_\downarrow : A_\uparrow$ shall be discussed. For Ni(111) ($\Upsilon_{Ni(111)}$=1.7) it does not correspond to that on Ni(100) ($\hbar\omega = 44eV$) found by Petrovykh et al. [15,17] (0.56) nor to that on Ni(110) (0.8) [16,17]. Therefore Υ may bank on the experimental parameters and/or the crystal face [18].

As it is shown below even the change of Υ in going from Ni(111) to *h*–BN/Ni(111) is influenced by more than one physical mechanism. The change in the area ratio $\Upsilon = A_\downarrow : A_\uparrow$ of 1.7 for Ni(111) to 1.1 for *h*–BN/Ni(111) bears information on the spin dependent electron transmission coefficient. The *h*–BN overlayer clearly alters the intensities of the spin polarized direct photoemission transitions at this particular place in k–space. This behaviour of decreasing Υ upon adsorption of a non-magnetic layer can be related to spin dependent scattering of the electrons during the propagation to the detector. The data shown in Figure 2 indicate that minority photoelectrons get much more efficiently scattered. This is in line with the Siegmann rule [19] stating that at low kinetic energies the electron scattering cross section is essentially proportional to the number of valence band d-holes of a material. Thus for ferromagnets where the d-holes are polarized a spin filter effect is expected and minority spins are scattered more efficiently. In the case of *h*–BN the Siegmann rule predicts no spin filtering since *h*–BN has no polarized d–shell. Therefore our finding of a strong asymmetry of the spin transition intensities calls for an extension of the Siegmann rule: it signals that spin filtering may also occur in non–magnetic overlayers that are coupled to a magnetic substrate. This coupling may be mediated by hybridisation of delocalized s–p states extending into the interface and/or by the surface umklapps of the *h*–BN grating on Ni(111) that increase the available phase space for electron hole pair excitations. Though the umklapps may play a crucial role for the understanding of the magnetic coupling across this interface it has to be emphasized that these very same umklapps may differently influence the matrix elements of the two spin channels shown in Fiure 2. Therefore the (essential) assumption of a constant matrix element for a quantitative determination of the spin scattering asymmetry may be hampered by surface umklapp processes.

In Figure 3 two dispersion plots of the s–p bands the of Ni and *h*–BN/Ni(111) in the sec-

ond surface Brillouin zone are shown. In order to make transitions from thermally populated states above the Fermi level visible, the data have been normalized with an experimentally determined Fermi function. The contrast is best near the Fermi level since there the broadening due to the hole lifetime is minimal. The steep slope of the bands indicates a large group velocity and identifies the bands to be s–p like. In Figure 3b) new features at azimuthal angles of $\pm 10°$ are resolved. These features have a maximum contrast at about 100 meV above the Fermi level. With the present data set the origin of these extra features can not be unambiguosly determined. It is likely that their origin is a surface umklapp. They may thus influence the matrix element of the photoemission process and alter the intensities of the s–p transitions at the Fermi level as shown in Figure 2. Before any quantitative statement on the spin scattering asymmetry such features have to be understood.

IV. CONCLUSIONS

In conclusion it has been shown how an advanced photoemission experiment may contibute to the better understanding of magnetic tunneling. It is of key importance to know the electronic states in k-space in order to comprehend electronic coupling across interfaces. For the model system of a layer of hexagonal boron nitiride on nickel it is demonstrated that a non-magnetic atomic grating may produce additional features on the Fermi surface. These surface umklapps are proposed to play a non-negligible role for the detailed understanding of tunneling in general and spin-polarized tunneling i.e. magnetic coupling in particular. For the understanding of intensity ratios and their exploitation for the determination of relevant physical quantities as e.g. spin scattering anisotropies, k–space has to be explored in detail. Support from high quality ab initio calculations is required.

ACKNOWLEDGMENTS

Support for the experiments from B. Schmid, P. Treier and W. Deichmann and financial support from the Schweizerischen Nationalfonds are gratefully acknowledged.

REFERENCES

[1] Physics Today, **45** April (1995).

[2] M.N. Baibich, J.M. Broto, A. Fert, F. Nguyen Van Dau, F. Petroff, P. Etienne, G. Creuzet, A. Friedrich and J. Chazelas, Phys. Rev. Lett.**61** (1988) 2472.

[3] P. Aebi, T.J. Kreutz, J. Osterwalder, R. Fasel, P. Schwaller and L. Schlapbach, Phys. Rev. Lett. **76** (1996) 1150.

[4] T. Greber, T.J. Kreutz and J. Osterwalder, Phys. Rev. Lett. **79** (1997) 4465.

[5] P. Aebi, J. Osterwalder, R. Fasel, D. Naumović and L. Schlapbach, Surf. Sci. **307-309** (1993) 917.

[6] A. Nagashima, N. Tejima, Y. Gamou, T. Kawai and C. Oshima, Phys. Rev. B **51** (1995) 4606.

[7] T. Greber, O. Raetzo, T. J. Kreutz, P. Schwaller, W. Deichmann, E. Wetli and J. Osterwalder, Rev. Sci. Instrum. **68** (1997) 4549.

[8] J. Osterwalder, T. Greber, J. Kröger, J. Wider, H.-J. Neff, F. Baumberger, M. Hoesch, W. Auwärter, R. Fasel and P. Aebi, these proceedings.

[9] Note: This statement has been corrected in comparison with the published version of this paper. Samples with a different inner potential do not allow to probe the same final state $\mathbf{k}_f$ at the same polar emission angle θ. This does, however, not affect the conclusions of the paper. We are grateful to M. Hengsberger who brougth the obscurity in the original version to our attention.

[10] W. Auwärter, T. J. Kreutz, T. Greber and J. Osterwalder, Surf. Sci. **429** (1999) 229.

[11] Y. Gamou, M. Terai, A. Nagashima, C. Oshima, Sci. Rep. RITU **A44** (1997) 211.

[12] T.J. Kreutz, T. Greber, P. Aebi, J. Osterwalder, Phys. Rev. B **58** (1998) 1300.

[13] M. Aeschlimann, M. Bauer, S. Pawlik, W. Weber, R. Burgermeister, D. Oberli and H.-C. Siegmann, Phys. Rev. Lett. **79** (1997) 5158.

[14] J.K. Grepstadt, B.J. Slagsvold and I. Bartos, J. Phys. F **12** (1982) 1679.

[15] D.Y. Petrovykh, K.N. Altmann, H. Höchst, M. Laubscher, S. Maat, G.J. Mankey and F. Himpsel, Appl. Phys. Lett. **73** (1998) 3459.

[16] T.J. Kreutz, P. Aebi, and J. Osterwalder, Sol. State Comm. **96** (1995) 339.

[17] F.J. Himpsel, K.N. Altmann, G.J. Mankey, J.E. Ortega and D.Y. Petrovykh, J. of Magnet. and Magnet. Mat. **200** (1999) 456.

[18] "In electron spectroscopies the intensity is – in contrast to energy, spin and momentum – a "bad quantum number" i.e. the matrix element and the transmission may vary from experiment to experiment. H.-C. Siegmann private Communication, Berlin 1994.

[19] H.-C. Siegmann, J. El. Spectr. and Rel. Phen. **68** (1994) 505.

TABLES

TABLE I. Parameters from the fits of four Gaussians to s-p bands at the Fermi level in the second surface Brillouin zone (see Figure 2). The k-values are calculated from $k = sin(\varphi) * k_{||}$, where φ is the angle measured from the $(\bar{1}10)$ plane and $k_{||} = sin(\theta)\sqrt{2m_e E_{kin}}/\hbar$, $(\theta = 78°)$.

Sample	$\delta k_{ex}(\AA^{-1})$	$\delta k_{\uparrow\uparrow}(\AA^{-1})$	$\gamma_{\uparrow}(\AA^{-1})$	$\gamma_{\downarrow}(\AA^{-1})$	$A_{\downarrow} : A_{\uparrow}$
Ni(111)	0.19(2)	0.83(2)	0.13(2)	0.17(2)	1.71(8)
h–BN/Ni(111)	0.16(2)	0.94(8)	0.12(2)	0.15(2)	1.08(5)

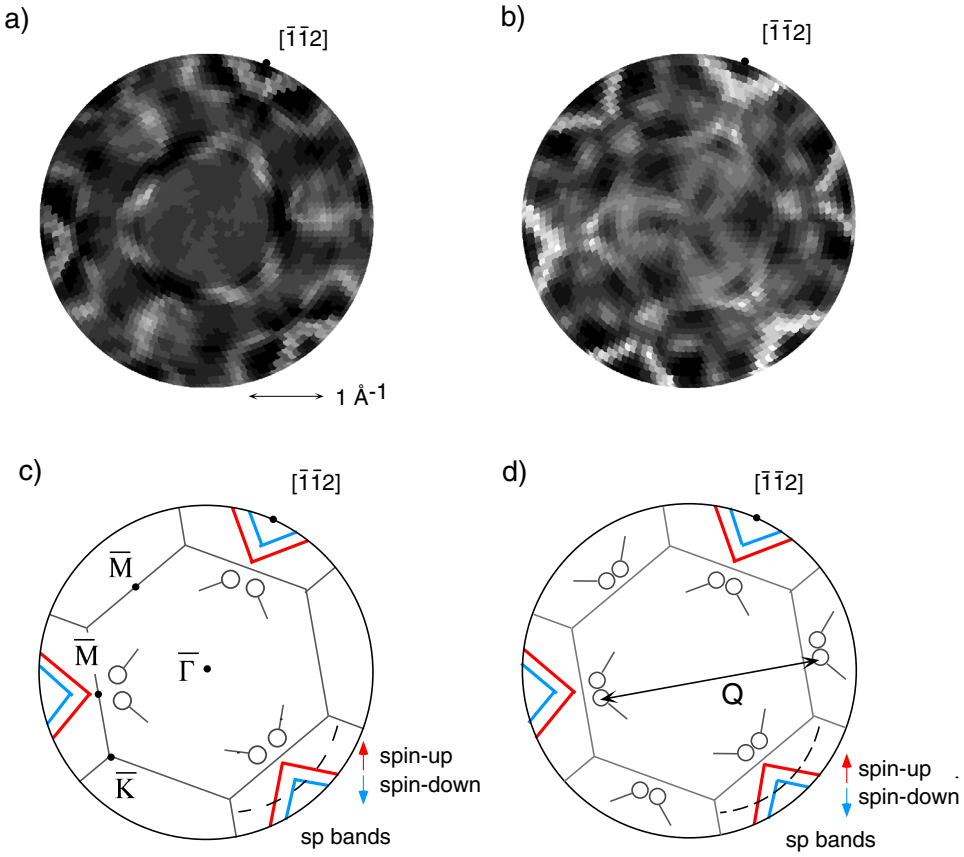

FIG. 1. Fermi surface maps as measured by angular resolved photoemission. The intensity on a linear gray scale (white means high intensity) is displayed as a function of $sin(\theta)$ and φ, θ being the polar and φ the azimuthal emission angle. The high symmetry direction $[\bar{1}\bar{1}2]$ is indicated. a) Ni(111) measured with He Iβ radiation ($k_{||} \leq 2.15\AA^{-1}$). b)h–BN/Ni(111)) measured with He Iα radiation ($k_{||} \leq 2.15\AA^{-1}$). c) Schematic diagram of the sampled k–space in a). The high symmetry points of the surface Brillouin zone are $\bar{\Gamma}, \bar{M}, \bar{K}$. The $\wedge$ wedge like features and the pairs of "signal disks" indicate s–p derived, spin–split bands. The dashed line across the wedges indicates the azimuthal cut in Figures 2 and 3. d) Schematic diagram of the sampled k–space in b). The three signal disk pairs appear shifted by a primitive reciprocal surface lattice vectors $|\mathbf{Q}| = \frac{2\pi}{a}\frac{2}{\sqrt{3}}$, where a is the surface lattice constant.

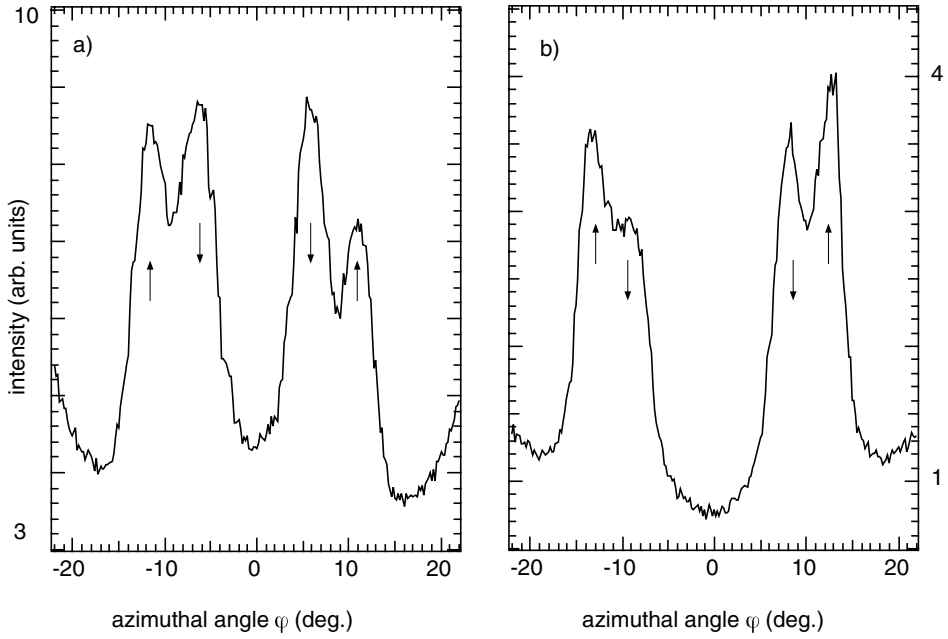

FIG. 2. Photoemission intensity at the Fermi level is plotted versus azimuthal angle. The polar emission angle ($\theta = 78°$) is kept constant. φ=0 is defined in the ($\bar{1}10$) plane. The arrows indicate the minority $\downarrow$ and majority $\uparrow$ bands, respectively. a) Ni(111) measured with He Iβ radiation. b)*h*–BN/Ni(111) measured with He Iα radiation. Note the strong change in the intensity ratio between minority and majority spin transitions.

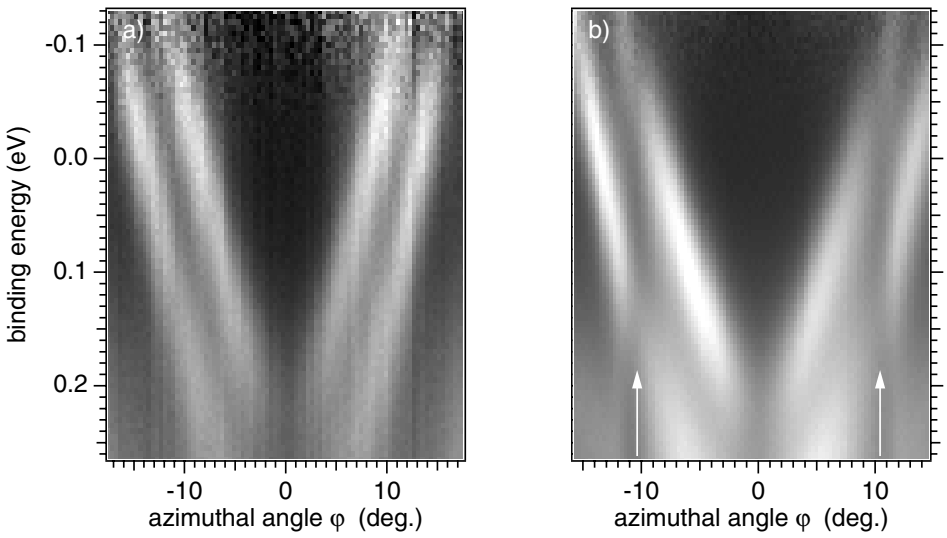

FIG. 3. Photoemission around the Fermi level. Dispersion plots along the azimuthal angles of Figure 2. The bright lines correspond to the spin–split s–p-bands. In order to visualize the bands above the Fermi level the data are normalized with an experimentally determined Fermi function. a) Ni(111) measured with He Iβ radiation. b)h–BN/Ni(111) measured with He Iα radiation. The arrows at $\varphi \sim \pm 10°$ indicate the positions where new spectral features (best seen 100 meV above the Fermi level) start to interfere with the 'native' s–p bands.